Photochemical & Photobiological Sciences

Nanosecond Transient Absorption Studies of the pH-Dependent Hydrated Electron Quenching by HSO_3^-

Journal:	*Photochemical & Photobiological Sciences*
Manuscript ID	PP-ART-02-2019-000063.R1
Article Type:	Paper
Date Submitted by the Author:	21-Feb-2019
Complete List of Authors:	Maza, William; US Naval Research Laboratory, Chemistry Division; National Research Council Breslin, Vanessa; National Research Council; US Naval Research Laboratory, Chemistry Division Plymale, Noah; National Research Council; US Naval Research Laboratory, Chemistry Division DeSario, Paul; US Naval Research Laboratory, Surface Chemistry Branch Epshteyn, Albert; US Naval Research Laboratory, Chemistry Division Owrutsky, Jeffrey; Naval Research Laboratory, Chemistry Division Pate, Bradford B.; US Naval Research Laboratory, Chemistry Division

Journal Name

ARTICLE

Nanosecond Transient Absorption Studies of the pH-Dependent Hydrated Electron Quenching by HSO_3^-.

Received 00th January 20xx,
Accepted 00th January 20xx

DOI: 10.1039/x0xx00000x

www.rsc.org/

William A. Maza,* [a] Vanessa M. Breslin,[a] Noah T. Plymale,[a] Paul A. DeSario,[b] Albert Epshteyn,[b] Jeffrey C. Owrutsky, * [b] and Bradford B. Pate* [b]

The large standard reduction potential of an aqueous solvated electron (e_{aq}^-, E° = -2.9 V) makes it an attractive candidate for reductive treatment of wastewater contaminants. Using transient absorption spectroscopy, the nanosecond to microsecond dynamics of e_{aq}^- generated from 10 mM solutions of Na_2SO_3 at pH 4 to 11 in H_2O and D_2O are characterized, resulting in the determination that between pH 4 and 9 it is the HSO_3^-, and not H^+ as previously postulated by others, that effectively quenches e_{aq}^-. The observed bimolecular quenching rate constant ($k = 1.2\times10^8\ M^{-1}\ s^{-1}$) for e_{aq}^- deactivation by HSO_3^- is found to be consistent with a Brönsted acid catalysis mechanism resulting in formation of H and SO_3^{2-}. A large solvent isotope effect is observed from the lifetimes of the e_{aq}^- in H_2O compared to D_2O ($k_{H2O}/k_{D2O} = 4.4$). In addition, the bimolecular rate constant for e_{aq}^- deactivation by DSO_3^- ($k = 2.7\times10^7\ M^{-1}\ s^{-1}$) is found to be an order of magnitude lower than by HSO_3^-. These results highlight the role of acids, such as HSO_3^-, in competition with organic contaminant targets for e_{aq}^- and, by extension, that knowledge of the pK_a of e_{aq}^- sources can be a predictive measure of the effective pH range for the treatment of wastewater contaminants.

Introduction

There are emerging reduction methodologies for the treatment of wastewater that take advantage of high-energy reducing species to decompose contaminants including long chain hydrocarbons, aromatics, and perfluoroalkanes.[1, 2] With a standard reduction potential (E°) of -2.9 V,[3-6] the hydrated electron (e_{aq}^-) is the most potent reducing agent that can exist in water; albeit short-lived, it may be useful in decomposing wastewater contaminants.[1, 2, 7-13] Herein we re-investigate the reason for the poor performance of advanced reduction water treatment processes involving the photochemical generation of e_{aq}^- from sulphite solutions at pH < 9, and show that HSO_3^-, which is present at pH values near the HSO_3^-/SO_3^{2-} pK_a, quenches the e_{aq}^- that is generated by irradiation of SO_3^{2-} at 266 nm. The rate constant for the quenching of e_{aq}^- by HSO_3^- is $1.2\times10^8\ M^{-1}\cdot s^{-1}$. The reaction occurs via a Brönsted acid catalysis mechanism to form $H^\cdot$ and SO_3^{2-}, with a large kinetic isotope effect (KIE = 4.4) for the e_{aq}^- quenching by HSO_3^- versus DSO_3^-. We attribute the large KIE to an order of magnitude decrease in the deactivation rate constant for the interaction of e_{aq}^- and DSO_3^-.

Like sulphite, UV-irradiation of certain anions (e.g., ferrocyanide, iodide, and hydroxide) is a known method of producing solvated electrons.[14] The characterization of the formation of e_{aq}^- and its subsequent interactions with water soluble species has been previously reported.[4, 15-17] The e_{aq}^- lifetime typically observed is on the order of microseconds and is sensitive to a variety of factors such as the ionic strength, pH, and the presence of electron acceptors.[15, 17-27] The rate constants for the interaction of e_{aq}^- with electron acceptors can vary between 10^4 to $10^{10}\ M^{-1}\cdot s^{-1}$.[16] For example, using nanosecond flash photolysis, Huang et al. reported a rate constant of $1.7\times10^7\ M^{-1}\cdot s^{-1}$ for the reduction of sodium perfluorooctanoate by photodetached e_{aq}^- from $K_4Fe(CN)_6$ solutions.[28] By the same technique, Levin et al. demonstrated that the rate constant for e_{aq}^- quenching by phosphate anions varies with pH and depends on the protonation state of the anion.[29] Sulphite (SO_3^{2-}), has been shown to be a particularly effective source of photochemically generated e_{aq}^- for the degradation of aqueous film-forming foams (AFFF) and its constituents (e.g., perfluoroalkylsulfonate), as well as other small molecule contaminants including pharmaceuticals.[30-37] The SO_3^{2-} system, as stated earlier, is limited in that it is only effective at pH > 8, unlike other systems that are active over broader pH ranges.[30-32, 36, 38] It has been shown that the degradative efficiency of SO_3^{2-} is improved in the presence of additives, like iodide, that increase pH upon irradiation and help maintain the solution conditions necessary for the SO_3^{2-} system to be effective.[34, 39]

[a] National Research Council, U.S. Naval Research Laboratory, Washington, D.C. 20375.
[b] Chemistry Division, U.S. Naval Research Laboratory, Washington, D.C. 20375.
* corresponding authors william.maza.ctr@nrl.navy.mil , bradford.pate@nrl.navy.mil , jeff.owrutsky@nrl.navy.mil .
Electronic Supplementary Information (ESI) available: additional data is available in the supplementary information. See DOI: 10.1039/x0xx00000x

The decline in degradative efficiency of the e_{aq}^- in Na_2SO_3 solutions at pH < 8 was previously attributed to competitive scavenging of the e_{aq}^- by protons (H^+) with increasing [H^+].[30, 31, 33] At pH values near the reported pK_a of 7.2 for the [HSO_3^-]/[SO_3^{2-}] equilibrium, however, the [H^+] is at least an order of magnitude less than [HSO_3^-] when the concentration of Na_2SO_3 is greater than 1 µM (Figure 1). Although Li et al. mention the potential role of HSO_3^- in deterring degradation of perfluoroalkyl contaminants, they did not explore its role in relation to H^+ any further.[40]

In this report, transient absorption spectroscopy is used to re-evaluate the roles of H^+ and HSO_3^- in scavenging photodetached e_{aq}^-. The nanosecond to microsecond dynamics of e_{aq}^- produced by UV irradiation (λ_{exc} = 266 nm) of Na_2SO_3 solutions are probed by monitoring the change in absorption of the e_{aq}^- at 790 nm ($\lambda_{cw\ probe}$ = 790 nm). The 790 nm probe is used to monitor the dynamics of the e_{aq}^- since the e_{aq}^- has a broad absorption between 400 nm and 1200 nm with a maximum at ca. 720 nm and a molar extinction coefficient, ε_{720nm}, of ca. 19000 M^{-1} cm^{-1}.[4, 41-43] The effect of pH on the lifetime of e_{aq}^- is investigated and the results are discussed in relation to the role of the [HSO_3^-]/[SO_3^{2-}] equilibrium.

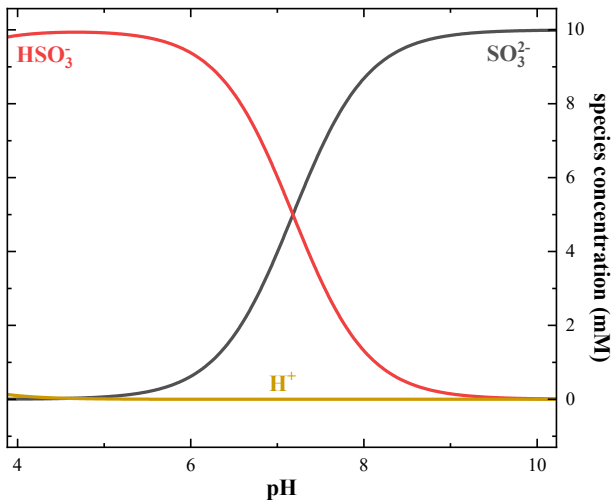

Figure 1. Concentration profiles of SO_3^{2-} (black line), HSO_3^- (red line) and H^+ (orange line) calculated as a function of pH for a 10 mM Na_2SO_3 solution using a pK_a of 7.2.[28, 43, 44]

Experimental

General Considerations: All chemicals, (Na_2SO_3 98% Alfa Aesar, KNO_3 ≥ 99% Sigma-Aldrich, and $K_4Fe(CN)_6{\cdot}3H_2O$ 99.95% Sigma-Aldrich) were used as received with no further purification. Stock solutions of 0.5 M Na_2SO_3 were freshly prepared in deionized water and stored under N_2. Samples of 10 mM Na_2SO_3 used for flash photolysis were prepared in a standard quartz cuvette (1 cm pathlength) from the 0.5 M stock, sealed with a rubber septum and parafilm, and purged with N_2 for at least 10 minutes. The sample pH was adjusted by addition of either $HClO_4$ or NaOH.

Flash Photolysis: The solvated aqueous electron, e_{aq}^-, dynamics were monitored on a flash photolysis system built in-house (~ 100 ns resolution) shown in Scheme 1. The fourth harmonic of a Continuum Minilite II Nd:YAG laser (λ_{exc} = 266 nm, 5 ns pulse width, 150 µJ per pulse output at sample) and the output of a continuous wave diode laser (λ_{probe} = 790 nm Thorlabs model CPS780S; λ_{probe} = 405 nm Power Technology model LDCU12/459U; λ_{probe} = 633 nm Spectra Physics HeNe model 102-4) were directed collinearly into the sample. The excitation and other stray light were filtered with a bandpass filter (785 nm centre, 405 nm centre, or 633 nm centre; 10 nm FWHM each) and the change in probe intensity monitored using a photomultiplier tube (Hamamatsu R375, 9 ns rise time, 70 ns transit time). The resultant analogue transient signal (each transient is the average of ~ 300 shots) was digitized on a Tektronix TDS 420A oscilloscope (200 MHz, 100 MS s^{-1} sampling rate).

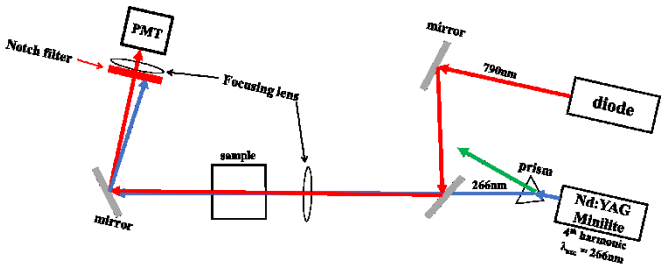

Scheme 1. Schematic of the laser flash photolysis system used to measure the nanosecond to microsecond transient absorption dynamics of e_{aq}^-.

Results and Discussion

Assignment of the transient signal as e_{aq}^-. Excitation of an anaerobic (nitrogen-purged) solution containing 10 mM Na_2SO_3 (pH ~ 9) with a 266 nm pulse produces a positive transient absorption signal at 790 nm that obeys first-order kinetics with a lifetime of 8.6 ± 0.2 µs (Figure 2). No detectible signal was observed at a probe wavelength of 405 nm, where the molar absorption of e_{aq}^- approaches zero (supplemental Figure S1). In contrast, when probing at 633 nm using a HeNe laser, we observed a signal amplitude commensurate with the expected absorption spectrum of e_{aq}^-.[4, 41, 42] The lifetimes obtained at both 790 and 633 nm are in very good agreement (Figure S1). To positively assign the signal observed at 790 nm as e_{aq}^-, KNO_3 was introduced to the solution resulting in a decrease in the e_{aq}^- lifetime with increasing [KNO_3] (Figure S3). Both the wavelength-dependence of the transient absorption and the effect of an electron scavenger on lifetime support the assignment of the transient signal observed at 790 nm as being due to the decay of photodetached e_{aq}^- (Figure 2).

pH effect on e_{aq}^- lifetime and the kinetic isotope effect. Upon formation of the e_{aq}^- the non-geminate e_{aq}^- + SO_3^- pair undergoes recombination according to:

$$SO_3^- + e_{aq}^- \xrightarrow{k_0} SO_3^{2-} \qquad \mathbf{1}$$

Additionally, the e_{aq}^- can interact with excess SO_3^{2-} according to **2** (supplemental information),

$$SO_3^{2-} + e_{aq}^- \xrightarrow{k_1} products \qquad \mathbf{2}$$

or interact with bisulphite, HSO_3^-, as shown in **3**.[43]

$$HSO_3^- + e_{aq}^- \xrightarrow{k_2} SO_3^{2-} + H^{\cdot} \qquad \mathbf{3}$$

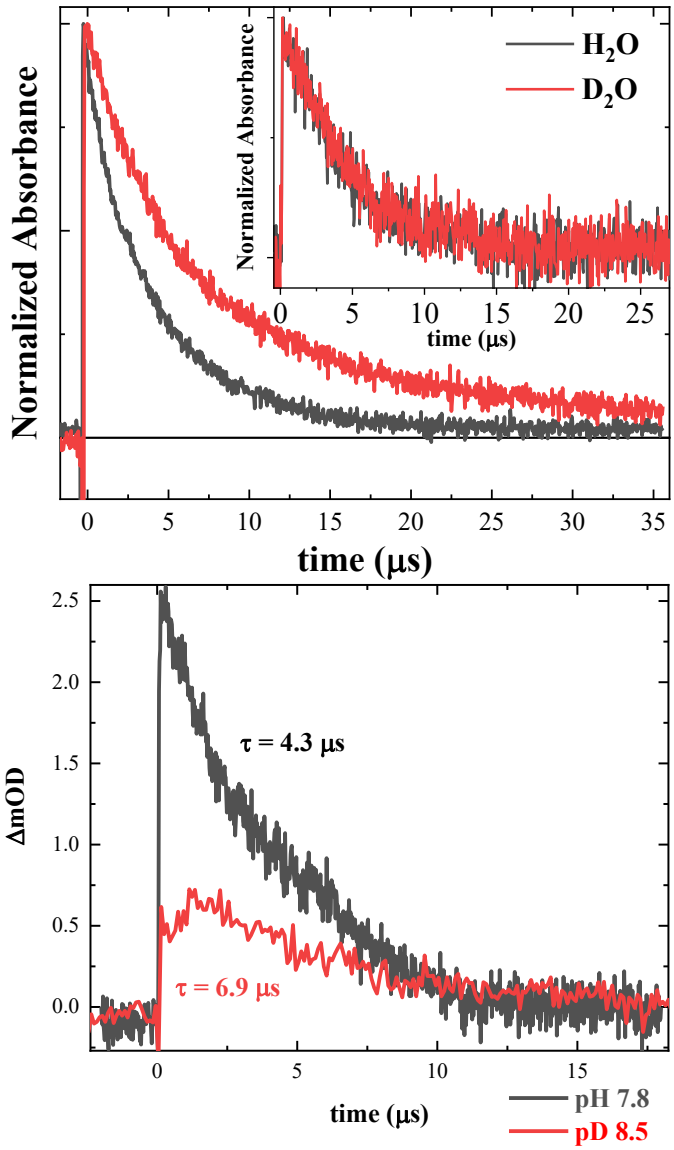

Figure 2. (Top panel) Normalized transient absorption signal at 790 nm containing 10 mM Na_2SO_3 at pH 9 and (inset) 40 μM $K_4Fe(CN)_6$ (enlarged figure shown in Figure S5) in H_2O (black line) and D_2O (red line). (Bottom panel) Transients were obtained from anaerobic solutions of 10 mM Na_2SO_3 at pH 7.83 in H_2O (black line) and pH 8.53 in D_2O (red line) where the concentration of HSO_3^- and DSO_3^- are approximately equivalent.

Transients obtained for 10 mM Na_2SO_3 solutions in H_2O at pH 4 – 11 reveal that both the signal amplitudes and lifetimes decrease with decreasing pH. The observed pH-dependent decrease in the e_{aq}^- lifetime may be a result of either efficient scavenging of the e_{aq}^- by H^+, or deactivation of e_{aq}^- via interaction with HSO_3^- (reaction **3**). The high $[HSO_3^-]$ as compared to the very small $[H^+]$ over this pH range (Figure 1) implicates HSO_3^- as the more likely primary quencher of e_{aq}^-. The concentration profile shown in Figure 1 is based on the reported pK_a value for the $[HSO_3^-]/[SO_3^{2-}]$ equilibrium (pK_a 7.2).[28, 43, 44]

To test this hypothesis, 10 mM Na_2SO_3 solutions were prepared in D_2O to determine whether there would be an observable difference in the e_{aq}^- lifetime in the presence of HSO_3^- vs. DSO_3^-. Indeed, a significant difference in the lifetime is observed for 10 mM Na_2SO_3 solutions in D_2O compared to H_2O under anaerobic conditions (Figure 2). The e_{aq}^- lifetime in D_2O (pD ~ 8.4) is 7.2 ± 0.7 μs compared to 4.8 ± 0.2 μs in H_2O (pH ~ 8.3). This difference in lifetime in D_2O compared to H_2O is just as pronounced at equal concentrations of HSO_3^- and DSO_3^- (~ 1 mM, Figure 2 bottom panel, Figure S7, the respective concentrations were estimated using data shown below) where the e_{aq}^- lifetimes are 4.3 μs in H_2O (pH 7.8) and 6.9 μs D_2O (pD 8.5).

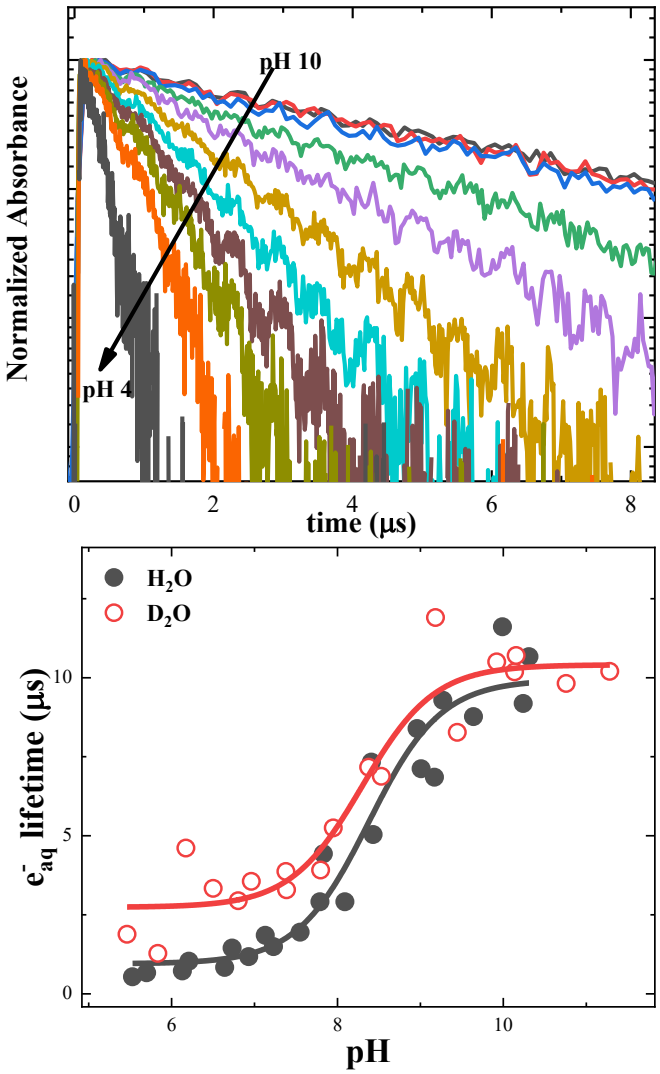

Figure 3. (Top) Normalized transient absorption traces obtained at 790 nm of e_{aq}^- photodetached from 10 mM Na_2SO_3 solutions at varying pH. (Bottom) Solvated electron lifetimes in H_2O (black closed circles) and D_2O (red open circles) obtained from mono-exponential fits of the transients. The solid black line represents a non-linear least squares fit of the lifetime data to equation **5**.

To support that the observed kinetic isotope effect (KIE) in Na_2SO_3 solutions prepared in H_2O and D_2O arises due to the reaction between the e_{aq}^- and HSO_3^- being the rate determining step (pH range of 4 to 10) we also probed solutions of $K_4Fe(CN)_6$

for comparison. In the absence of a protonated species the e_{aq}^- transient generated from solutions of $K_4Fe(CN)_6$, solutions prepared in H_2O and D_2O should have identical quenching rates.[45-47] This was indeed the case (Figure 2, inset and Figure S8). Mono-exponential fits of the e_{aq}^- transients in 40 µM $K_4Fe(CN)_6$ prepared in H_2O and D_2O (pH, pD ~7) indicated e_{aq}^- lifetimes of 4.6 ± 0.8 µs and 4.1 ± 0.6 µs, respectively.

The role of HSO_3^- is more evident from the differences in the signals observed for e_{aq}^- generated from 10 mM and 500 mM solutions of Na_2SO_3 at pH 7 (Figure S9). At pH 7, the e_{aq}^- lifetime in a 10 mM solution is ~1.5 µs, whereas the lifetime in a 500 mM Na_2SO_3 solution was found to be at or below the detection limit of our instrumentation ($\tau_{obs} \leq 100$ ns). These results suggest that in a 500 mM Na_2SO_3 solution at pH 7 the concentration of HSO_3^- is sufficiently high that the reaction described by reaction **3** dominates all other processes (discussed further below).

A model was developed in which the lifetime of the e_{aq}^- depends on both the recombination of e_{aq}^- with SO_3^- and the deactivation reaction between e_{aq}^- and SO_3^{2-} or HSO_3^- as suggested in reactions **1**, **2**, and **3**. The rate expression which includes these irreversible processes yields the following expression for the observed lifetime:

$$\tau = (k_o[SO_3^-] + k_1[SO_3^{2-}] + k_2[HSO_3^-])^{-1} \qquad \mathbf{4}$$

Equation **4** can be rewritten (see supplemental for derivation) in terms of the initial SO_3^{2-} concentration, $[SO_3^{2-}]_o$, the pK_a of the HSO_3^-/SO_3^{2-} equilibrium, the solution pH, and the reciprocal of the sum $k_1[SO_3^-] + k_o[SO_3^{2-}]$ represented as τ_o (i.e., the lifetime of the e_{aq}^- at high pH where the concentration of HSO_3^- is negligible) to give equation **5**:

$$\tau = \frac{10^{pH}+10^{pK_a}}{k_2 10^{pK_a}[SO_3^{2-}]_o + \frac{10^{pH}+10^{pK_a}}{\tau_o}} \qquad \mathbf{5}$$

Due to its blue shifted charge-transfer-to-solvent transition relative to SO_3^{2-}, absorption of the incident 266 nm laser pump pulse by HSO_3^- is negligible.[43] Therefore, the contribution to e_{aq}^- formation by direct excitation of HSO_3^- is neglected.

The e_{aq}^- lifetime data obtained as a function of the solution pH was fit to equation **5** (Figure 3) resulting in pK_a, τ_o, and k_2 values of 7.2 ± 0.1, 9.8 ± 0.1 µs, and (1.2 ± 0.3)x10^8 M^{-1} s^{-1}, respectively. The pK_a value obtained from the fit is in excellent agreement with results from the ground state absorption (pK_a = 7.1 ± 0.1, Figure S10) and the reported pK_a value of 7.2.[28, 43, 44] These values for pK_a, k_2, and τ_o represent the average of multiple data sets. It should be noted that the value obtained for k_2 is an order of magnitude greater than that reported by Hayon et al. (i.e., 2x10^7 M^{-1} s^{-1}).[43] Similarly, fits of the e_{aq}^- lifetimes in D_2O as a function of pD yield pK_a, τ_o, and k_2 values of 7.8 ± 0.1, 10.4 ± 0.9 µs, and (2.7 ± 0.02)x10^7 $M^{-1}\cdot s^{-1}$, respectively.

The e_{aq}^- lifetime trend observed between H_2O and D_2O seem counterintuitive for a shift in the HSO_3^-/SO_3^{2-} pK_a from 7.2 to 7.8, respectively. For example, at pH 8 a shorter lifetime is expected in D_2O relative to H_2O given the higher concentration of H/DSO_3^- expected in D_2O compared to H_2O (Figure **S7**). This is indeed the predicted outcome according to equation **5** if k_2 were the same in D_2O and H_2O (Figure **S11**). The expected decrease in e_{aq}^- lifetime at pD 8 resulting from the shift in pK_a is countermanded, however, by the 4-fold decrease of k_2 in D_2O which results in a longer lifetime in heavy water.

Mechanism of quenching of e_{aq}^- by HSO_3^-. Conversion of e_{aq}^- to $H^\cdot$ by reaction with a protonated acid, BH, in aqueous solutions is known to occur in the presence of Brönsted acids by a general acid catalysis mechanism according to equation **6**.[48]

$$BH \quad + e_{aq}^- \rightarrow H + B^- \qquad \mathbf{6}$$

Here, BH is a protic acid and B^- is the conjugate base. Figure 4 shows the strong correlation between the e_{aq}^- deactivation rate constant (equivalent to k_2 here) and the acid pK_a according to the Brönsted equation below:

$$\log\left(\frac{k_2}{p}\right) = \log\left[G_A\left(\frac{qK_a}{p}\right)^{\alpha}\right] \qquad \mathbf{7}$$

where p and q correspond to the number of dissociable protons available to the acid and the number of equivalent protonation sites available to the conjugate base, respectively. G_A and α are constants specific to similar types of acids and are sensitive to the acid catalyzed reaction. It is believed that the reaction is mediated by neighboring water.[49] For example, efficient deactivation of e_{aq}^-, generating $H^\cdot$, has been observed in the presence of H_3PO_4, $H_2PO_4^-$, CH_3COOH, and HCOOH.[49, 50] Rate constants corresponding to the reaction of e_{aq}^- with phosphate acids depend on its level of protonation. Specifically, the rate constant for the reaction between e_{aq}^- and H_3PO_4 has been reported as 1x10^9 $M^{-1}\cdot s^{-1}$, whereas the rate constant for the reaction between e_{aq}^- and $H_2PO_4^-$ has been reported to be between 10^6 and 10^7 $M^{-1}\cdot s^{-1}$.[49]

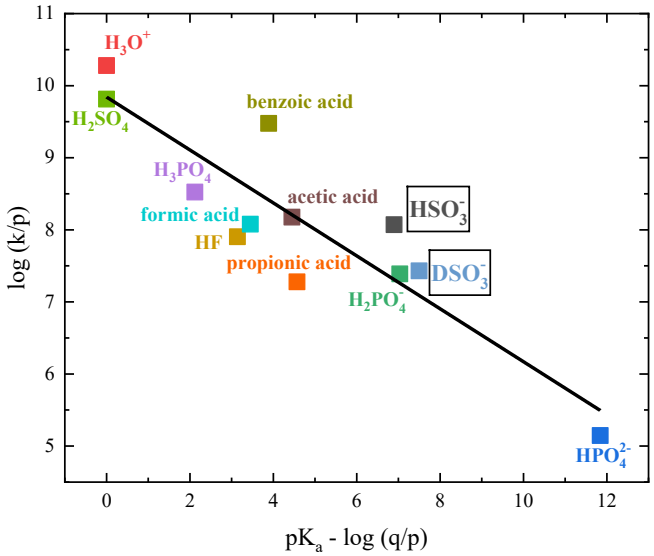

Figure 4. Brönsted law for the conversion of e_{aq}^- to H by HSO_3^- compared to other protic acids. Solid line represents the best fit to equation **7**. The values used for the points present in the plot were obtained from references [48-55]. The HSO_3^- and DSO_3^- points are based on this work.

The interaction between e_{aq}^- and HSO_3^- or DSO_3^- has a large kinetic isotope effect (KIE). The ratio of the rate constants, $k_2(H_2O)/k_2(D_2O)$, is ~4.4. This result is similar to the KIE between e_{aq}^- and H_3O^+/D_3O^+, as well as between e_{aq}^- and ammonium, which were previously reported to be ~4.[56] Alternatively, the difference between the rate constants for HSO_3^- versus DSO_3^- is greater than the factor of two difference between the deactivation of e_{aq}^- by H_2SO_4 (1.3×10^{10} $M^{-1}\cdot s^{-1}$) and D_2SO_4 (6.3×10^9 $M^{-1}\cdot s^{-1}$).[57]

The deactivation of e_{aq}^- can be described, according to Anbar[15], as an electron transfer reaction to HSO_3^-, generating a HSO_3^{2-} transient, which then decomposes to SO_3^{2-} and $H^\cdot$ (Eq. **8a**).

$$HSO_3^- + e_{aq}^- \rightarrow [HSO_3^{2-}] \rightarrow H^\cdot + SO_3^{2-} \qquad \textbf{8a}$$

Alternatively, Han et al. have suggested that the deactivation of e_{aq}^- may occur by direct H^+ transfer to e_{aq}^- (Eq. **8b**).[58]

$$e_{aq}^- + HSO_3^- \rightarrow \left[e_{aq}^- \cdots H^+ \cdots SO_3^{2-}\right] \rightarrow H^\cdot + SO_3^{2-} \qquad \textbf{8b}$$

The precise mechanism for the quenching of e_{aq}^- by HSO_3^- is difficult to assign unambiguously with the data presented here. However, the large KIE suggests reaction **8b** as the more probable pathway. In fact, molecular dynamics simulations performed by Marsalek, et al.[59] indicate that the reaction between e_{aq}^- + H_3O^+ occurs by proton shuttling via the hydrogen-bonding network surrounding a contracted e_{aq}^- cavity, strongly supporting a proton-transfer mechanism such as that given by reaction **8b**. Additionally, Ma, et al.[60] have demonstrated a blue shift in the transient absorption maxima (occurring within 10 ps) of the e_{aq}^- with increasing $HClO_4$ concentration and proposed that this blue shift is indicative of the formation of a $H_3O^+\cdots e_{aq}^-$ pair. By correlation, the fast (ps) formation of an $e_{aq}^-\cdots HSO_3^-$ pair may explain the similar KIE between H_3O^+ and HSO_3^- observed on the microsecond timescale.

Finally, the rate constants measured for reactions **1**, **2,** and **3** are 1 – 2 orders of magnitude smaller than the diffusional rate constants (shown in the supplemental), indicating that the observed quenching of e_{aq}^- is not diffusion limited. This is not uncommon and has been observed for a number of other inorganic ions.[15, 17]

Summary and Conclusions

The origin of the poor performance of advanced reduction processes involving the photochemical production of e_{aq}^- from sulphite solutions at pH < 9 has been re-examined. Based on the evidence presented, we postulate that it is the species HSO_3^- (formed at pH values near the HSO_3^-/SO_3^{2-} pK_a) that quenches e_{aq}^- generated by the irradiation of SO_3^{2-} at 266 nm. The rate constant for quenching of e_{aq}^- by HSO_3^- is 1.2×10^8 $M^{-1}\cdot s^{-1}$ and we propose that the reaction resulting in formation of H and SO_3^{2-} occurs via a Brönsted acid catalysis mechanism, which is consistent and in good agreement with the general trend of the rate of deactivation of e_{aq}^- described by the Brönsted model for other protic acids. A large kinetic isotope effect (KIE = 4.4) is observed for the e_{aq}^- quenching by HSO_3^- versus DSO_3^- and is attributed to a decrease in the deactivation rate constant corresponding to the DSO_3^- + e_{aq}^- interaction by an order of magnitude. Consequently, as has been shown by others, the presence of HSO_3^- imposes restrictions on the effective pH range in which the SO_3^{2-} advanced reduction system can function efficiently. Knowledge of the acid dissociation constant (pK_a) can serve as a predictor of the efficacy of other inorganic salts known to generate solvated electrons upon UV-irradiation in processes where control of pH is an engineering challenge.

Conflicts of interest

The authors have no conflicts of interest to declare.

Acknowledgements

The authors acknowledge support for this work provided for by the Office of Naval Research. WAM, VMB, and NTP would like to thank the National Research Council for administrating their postdoctoral research fellowships.

Notes

‡ Additional data provided in a separate supplemental information document available for free at pubs.rsc.org.

References

1. B. P. Vellanki, B. Batchelor and A. Abdel-Wahab, Advanced Reduction Processes: A New Class of Treatment Processes, *Environ. Eng. Sci.*, 2013, **30**, 264-271.
2. S. Y. Yang, Y. T. Zhang and D. Zheng, Advanced Reduction Processes: A Novel Technology for Water Treatment, *Prog. Chem.*, 2016, **28**, 934-941.
3. J. Baxendale, *Addendum: Redox Potential and Hydration Energy of the Hydrated Electron*, Univ. of Manchester, Eng., 1964.
4. G. V. Buxton, C. L. Greenstock, W. P. Helman and A. B. Ross, Critical-Review of Rate Constants for Reactions of Hydrated Electrons, Hydrogen-Atoms and Hydroxyl Radicals ($^\cdot OH/^\cdot O^-$) in Aqueous-Solution, *J. Phys. Chem. Ref. Data*, 1988, **17**, 513-886.
5. R. F. Gould, ed., *Solvated electron; a symposium sponsored by the Division of Physical Chemistry at the 150th Meeting of the American Chemical Society*, American Chemical Society, Washington, DC, 1965.
6. R. A. Marcus, Theory of Electron-Transfer Reaction Rates of Solvated Electrons, *J. Chem. Phys.*, 1965, **43**, 3477-&.
7. J. J. L. Penalver, C. V. G. Pacheco, M. S. Polo and J. R. Utrilla, Degradation of Tetracyclines in Different Water Matrices by Advanced Oxidation/Reduction Processes Based on Gamma Radiation, *J. Chem. Technol. Biot.*, 2013, **88**, 1096-1108.

8. X. Liu, S. Yoon, B. Batchelor and A. Abdel-Wahab, Degradation of Vinyl Chloride (VC) by the Sulfite/UV Advanced Reduction Process (ARP): Effects of Process Variables and a Kinetic Model, *Sci. Total. Environ.*, 2013, **454**, 578-583.
9. B. P. Vellanki and B. Batchelor, Perchlorate Reduction by the Sulfite/Ultraviolet Light Advanced Reduction Process, *J. Hazard. Mater.*, 2013, **262**, 348-356.
10. X. Liu, S. Yoon, B. Batchelor and A. Abdel-Wahab, Photochemical Degradation of Vinyl Chloride with an Advanced Reduction Process (ARP) - Effects of Reagents and pH, *Chem. Eng. J.*, 2013, **215**, 868-875.
11. M. Trojanowicz, A. Bojanowska-Czajka, I. Bartosiewicz and K. Kulisa, Advanced Oxidation/Reduction Processes Treatment for Aqueous Perfluorooctanoate (PFOA) and Perfluorooctanesulfonate (PFOS) - A Review of Recent Advances, *Chem. Eng. J.*, 2018, **336**, 170-199.
12. M. Qiwen, K. H. Kim and I. Han, Correlation Analysis of Pollutant Factors Influencing the Sulfite/UV-L Advanced Reduction Process, *KSCE J. Civ. Eng.*, 2018, **22**, 475-481.
13. M. Trojanowicz, K. Bobrowski, B. Szostek, A. Bojanowska-Czajka, T. Szreder, I. Bartoszewicz and K. Kulisa, A Survey of Analytical Methods Employed for Monitoring of Advanced Oxidation/Reduction Processes for Decomposition of Selected Perfluorinated Environmental Pollutants, *Talanta*, 2018, **177**, 122-141.
14. M. C. Sauer, R. A. Crowell and I. A. Shkrob, Electron Photodetachment from Aqueous Anions. 1. Quantum Yields for Generation of Hydrated Electron by 193 and 248 nm Laser Photoexcitation of Miscellaneous Inorganic Anions, *J. Phys. Chem. A.*, 2004, **108**, 5490-5502.
15. M. Anbar, in *Solvated Electron*, American Chemical Society, Washington, D.C., 1965, vol. 50, ch. 6, pp. 55-81.
16. M. Anbar and P. Neta, Tables of Bimolecular Rate Constants of Hydrated Electrons Hydrogen Atoms and Hydroxyl Radicals with Inorganic and Organic Compounds, *Int. J. Appl. Radiat. Is.*, 1965, **16**, 227-&.
17. M. Anbar, The Reactions of Hydrated Electrons with Inorganic Compounds, *Q. Rev. Chem. Soc.*, 1968, **22**, 578-598.
18. E. J. Hart and J. W. Boag, Absorption Spectrum of the Hydrated Electron in Water and in Aqueous Solutions, *J. Am. Chem. Soc.*, 1962, **84**, 4090-4095.
19. M. Anbar and E. J. Hart, in *Radiation Chemistry*, American Chemical Society, Washington, D.C., 1968, vol. 81, ch. 6, pp. 79-94.
20. M. Anbar, in *Advances in Physical Organic Chemistry*, ed. V. Gold, Academic Press, 1969, vol. 7, pp. 115-151.
21. M. Gratzel and J. K. Thomas, Laser Photoionization in Micellar Solutions - Fate of Photoelectrons, *J. Phys. Chem.*, 1974, **78**, 2248-2254.
22. C. D. Borsarelli, S. G. Bertolotti and C. M. Previtali, Thermodynamic Changes Associated with the Formation of the Hydrated Electron After Photoionization of Inorganic Anions: A Time-Resolved Photoacoustic Study, *Photochem. Photobiol. Sci.*, 2003, **2**, 791-795.
23. R. Boch, M. K. Whittlesey and J. C. Scaiano, Laser-Induced Photoionization of Aromatic Ketones in Anionic Micellar Solutions, *J. Phys. Chem.*, 1994, **98**, 7854-7857.
24. O. Horvath and K. L. Stevenson, Micellar Effects on Photoinduced Redox Reactions of $Fe(bpy)_2(CN)_2$, *J Photoch Photobio A*, 1999, **120**, 185-190.
25. K. L. Stevenson, G. A. Papadantonakis and P. R. LeBreton, Nanosecond UV Laser Photoionization of Aqueous Tryptophan: Temperature Dependence of Quantum Yield, Mechanism, and Kinetics of Hydrated Electron Decay, *J. Photochem. Photobiol. A.*, 2000, **133**, 159-167.
26. R. J. Hamers, J. A. Bandy, D. Zhu and L. Zhang, Photoemission From Diamond Films and Substrates into Water: Dynamics of Solvated Electrons and Implications for Diamond Photoelectrochemistry, *Faraday Discuss.*, 2014, **172**, 397-411.
27. D. Zhu, L. Zhang, R. E. Ruther and R. J. Hamers, Photo-Illuminated Diamond as a Solid-State Source of Solvated Electrons in Water for Nitrogen Reduction, *Nat. Mater.*, 2013, **12**, 836.
28. L. Huang, W. B. Dong and H. Q. Hou, Investigation of the Reactivity of Hydrated Electron Toward Perfluorinated Carboxylates by Laser Flash Photolysis, *Chem. Phys. Lett.*, 2007, **436**, 124-128.
29. P. P. Levin, O. N. Brzhevskaya and O. S. Nedelina, Kinetics of Hydrated Electron Reactions with Phosphate Anions: A Laser Photolysis Study, *Russ. Chem. Bull.*, 2007, **56**, 1325-1328.
30. Y. R. Gu, W. Y. Dong, C. Luo and T. Z. Liu, Efficient Reductive Decomposition of Perfluorooctanesulfonate in a High Photon Flux UV/Sulfite System, *Environ. Sci. Technol.*, 2016, **50**, 10554-10561.
31. Y. R. Gu, T. Z. Liu, H. J. Wang, H. L. Han and W. Y. Dong, Hydrated Electron Based Decomposition of Perfluorooctane Sulfonate (PFOS) in the VUV/Sulfite System, *Sci. Total. Environ.*, 2017, **607**, 541-548.
32. Y. R. Gu, T. Z. Liu, Q. Zhang and W. Y. Dong, Efficient Decomposition of Perfluorooctanoic Acid by a High Photon Flux UV/Sulfite Process: Kinetics and Associated Toxicity, *Chem. Eng. J.*, 2017, **326**, 1125-1133.
33. Z. Song, H. Q. Tang, N. Wang and L. H. Zhu, Reductive Defluorination of Perfluorooctanoic Acid by Hydrated Electrons in a Sulfite-Mediated UV Photochemical System, *J. Hazard. Mater.*, 2013, **262**, 332-338.
34. K. E. Yu, X. C. Li, L. W. Chen, J. Y. Fang, H. L. Chen, Q. B. Li, N. P. Chi and J. Ma, Mechanism and Efficiency of Contaminant Reduction by Hydrated Electron in the Sulfite/Iodide/UV Process, *Water. Res.*, 2018, **129**, 357-364.
35. X. W. Liu, T. Q. Zhang, L. L. Wang, Y. Shao and L. Fang, Hydrated Electron-Based Degradation of Atenolol in Aqueous Solution, *Chem. Eng. J.*, 2015, **260**, 740-748.
36. C. S. Liu, K. Shih and F. Wang, Oxidative Decomposition of Perfluorooctanesulfonate in Water by Permanganate, *Sep. Purif. Technol.*, 2012, **87**, 95-100.
37. S. Nawaz, N. S. Shah, J. A. Khan, M. Sayed, A. H. Al-Muhtaseb, H. R. Andersen, N. Muhammad, B. Murtaza and H. M. Khan, Removal Efficiency and Economic Cost Comparison of Hydrated Electron-Mediated Reductive

Pathways for Treatment of Bromate, *Chem. Eng. J.*, 2017, **320**, 523-531.

38. V. Ochoa-Herrera, R. Sierra-Alvarez, A. Somogyi, N. E. Jacobsen, V. H. Wysocki and J. A. Field, Reductive Defluorination of Perfluorooctane Sulfonate, *Environ. Sci. Technol.*, 2008, **42**, 3260-3264.
39. H. Park, C. D. Vecitis, J. Cheng, N. F. Dalleska, B. T. Mader and M. R. Hoffmann, Reductive Degradation of Perfluoroalkyl Compounds with Aquated Electrons Generated from Iodide Photolysis at 254 nm, *Photochem. Photobiol. Sci.*, 2011, **10**, 1945-1953.
40. X. Li, J. Fang, G. Liu, S. Zhang, B. Pan and J. Ma, Kinetics and efficiency of the hydrated electron-induced dehalogenation by the sulfite/UV process, *Water Res.*, 2014, **62**, 220-228.
41. E. J. Hart, B. Michael and K. H. Schmidt, Absorption Spectrum of e_{aq}^-in the Temperature Range -4 to 390°, *J. Phys. Chem.*, 1971, **75**, 2798-2805.
42. L. M. Dorfman, F. Jou and R. Wageman, Solvated Electron Solvent Dependence of the Optical Absorption Spectrum of the solvated Electron, *Berich. Bunsen. Gesell.*, 1971, **75**, 681-685.
43. E. Hayon, A. Treinin and J. Wilf, Electronic-Spectra, Photochemistry, and Autoxidation Mechanism of Sulfite-Bisulfite-Pyrosulfite Systems - SO_2^-, SO_3^-, SO_4^-, and SO_5^- Radicals, *J. Amer. Chem. Soc.*, 1972, **94**, 47-57.
44. L. Dogliotti and E. Hayon, Flash Photolysis Study of Sulfite Thiocyanate and Thiosulfate Ions in Solution, *J. Phys. Chem.*, 1968, **72**, 1800-1807.
45. I. M. Kolthoff and W. J. Tomsicek, The Fourth Ionization Constant of Ferrocyanic Acid, *J. Phys. Chem.*, 1934, **39**, 955-958.
46. G. I. H. Hanania, D. H. Irvine, W. A. Eaton and P. George, Thermodynamic Aspects of the Potassium Hexacyano-Ferrate(III)-(II) System. II. Reduction Potential, *J. Phys. Chem.*, 1967, **71**, 2022-2030.
47. A. E. Martell and R. M. Smith, *Critical Stability Constants*, Plenum Press, New York, N.Y., 1974.
48. J. Rabani, in *Solvated Electron*, 1965, vol. 50, ch. 17, pp. 242-252.
49. J. Jortner, M. Ottolenghi, J. Rabani and G. Stein, Conversion of Solvated Electrons into Hydrogen Atoms in Photo- and Radiation Chemistry of Aqueous Solutions, *J. Chem. Phys.*, 1962, **37**, 2488-&.
50. S. Gordon, E. J. Hart, M. S. Matheson, J. Rabani and J. K. Thomas, Reaction Constants of the Hydrated Electron, *J. Am. Chem. Soc.*, 1963, **85**, 1375-1377.
51. L. M. Dorfman and I. A. Taub, Pulse Radiolysis Studies. III. Elementary Reactions in Aqueous Ethanol Solution, *J. Am. Chem. Soc.*, 1963, **85**, 2370-2374.
52. G. Grabner, N. Getoff and F. Schwörer, Pulsradiolyse von H_3PO_4, $H_2PO_4^-$, HPO_4^{2-} und $P_2O_7^{4-}$ in Wässriger Lösung—I. Geschwindigkeitskonstanten der reaktionen mit den primärprodukten der wasserradiolyse, *Int. J. Rad. Phys. Chem.*, 1973, **5**, 393-403.
53. G. Phillips, D. Power and M. Sewart, Effects of γ-Irradiation on Sulphonamides, *Radiat. Res.*, 1973, **53**, 204-215.
54. O. Mićić and V. Marković, Rates of Hydrated Electron Reactions with Undissociated Carboxylic Acids, *Int. J. Rad. Phys. Chem.*, 1972, **4**, 43-49.
55. M. Anbar, M. Bambenek and A. B. Ross, *Selected Specific Rates of Reactions of Transients from Water in Aqueous Solution*, U.S. National Bureau of Standards, Washington, D.C., 1973.
56. M. Anbar and D. Meyerstein, Isotope Effects in the Radiolysis and Photolysis of H_2O—D_2O Mixtures, *J. Phys. Chem.*, 1965, **69**, 698-700.
57. D. M. Bartels, M. T. Craw, P. Han and A. D. Trifunac, H/D Isotope Effects in Water Radiolysis .1. Chemically-Induced Dynamic Electron Polarization in Spurs, *J. Phys. Chem.*, 1989, **93**, 2412-2421.
58. P. Han and D. M. Bartels, H/D Isotope Effects in Water Radiolysis .4. The Mechanism of $H_{aq}^- \leftrightarrows e_{aq}^-$ Interconversion, *J. Phys. Chem.*, 1992, **96**, 4899-4906.
59. O. Marsalek, T. Frigato, J. VandeVondele, S. E. Bradforth, B. Schmidt, C. Schütte and P. Jungwirth, Hydrogen forms in water by proton transfer to a distorted electron, *J. Phys. Chem. B*, 2009, **114**, 915-920.
60. J. Ma, U. Schmidhammer and M. Mostafavi, Direct evidence for transient pair formation between a solvated electron and H_3O^+ observed by picosecond pulse radiolysis, *J. Phys. Chem. Lett.*, 2014, **5**, 2219-2223.

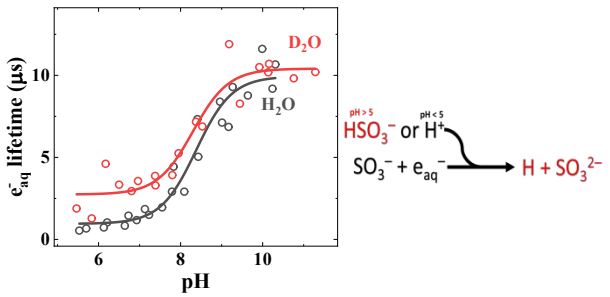

Hydrated electron lifetimes in photodetached sulfite solutions at intermediate pH (5-10) are limited by HSO_3^- rather than proton (H^+) quenching